1 A Single Atom

Learning Objectives

- Discuss the Coulomb interaction, the spin-orbit coupling, and the hyperfine coupling as the three effects that determine atomic structure.
- Highlight the importance of the separation of energy scales of these three effects.
- Introduce different atomic structures of alkali-metal, alkaline-earth-metal, and magnetic atoms.
- Introduce the long-lived excited states in alkaline-earth atoms, and their applications, such as to atomic optical clocks.
- Discuss the Zeeman structure of atoms in a magnetic field.
- Discuss the idea of magnetic trapping, which can naturally lead to the emergence of a synthetic gauge field.
- Introduce the scalar light shift and its applications, such as laser trapping, optical lattices, and laser cooling.
- Introduce the vector light shift and its applications, such as the light-induced Zeeman field and synthetic spin-orbit coupling.
- Discuss the synthetic spin-orbit coupling and various kinds of gauge fields generated by the vector light shift.
- Introduce the basic idea of the stimulated Raman adiabatic passage.

1.1 Electronic Structure

Let us first consider a general Hamiltonian of Z electrons moving around a nucleus that contains the Coulomb interaction, the spin-orbit coupling, and the hyperfine coupling. These are the three effects that determine the electronic structure of an atom. Here we should emphasize the important role of the separation of energy scales; that is to say, the typical energy scales of these three terms are quite different. Thanks to the separation of energy scales, we can analyze them one by one, which enables us to obtain a clear picture of the electron structure.

Coulomb Interaction between Electron and Nucleus. Each electron moves around the nucleus with an attractive Coulomb interaction between the electron and the nucleus, which is described by

https://doi.org/10.1017/9781108595216.002 Published online by Cambridge University Press

$$\hat{H}_0 = \sum_{i=1}^{Z} \left(-\frac{\hbar^2 \nabla_i^2}{2m^*} + V_{\rm ei}(\mathbf{r}_i) \right), \tag{1.1}$$

where $i = 1, \ldots, Z$ labels the electrons; $\mathbf{r}_i$ labels the coordinate of electron centering at the nucleus; $m^* = mM/(m+M)$ is the reduced mass, where m is the electron mass and M is the nucleus mass; $V_{\rm ei}(\mathbf{r}) = -Z\kappa/r$ is the Coulomb potentials between the electron and the nucleus, where $\kappa = e^2/(4\pi\epsilon_0)$; e is the electron charge; and ϵ_0 is the vacuum permittivity. The eigenstates are characterized by three quantum numbers (n, l, m). Usually for the spherical symmetric potential, because of the $SO(3)$ rotational symmetry, the energy spectrum only depends on n and l and does not depend on m. However, for the $1/r$ Coulomb potential, such as with a hydrogen atom, the eigenspectrum is

$$E = -\frac{m^* Z^2 \kappa^2}{2\hbar^2 n^2}, \tag{1.2}$$

which only depends on the principal quantum number n and is independent of angular momentum quantum number l; l can take integer values from 0 to $n-1$. This extra degeneracy is a consequence of $1/r$ potential, which leads to an $SO(4)$ symmetry larger than the three-dimensional rotational symmetry [102]. The separation of these energy levels is of the order of electron volts ($\sim 10^{14}$Hz) because it originates from the Coulomb interaction. The energy levels, usually named as the term-diagrams, are schematized in Figure 1.1, where $1, 2, 3, \ldots$ label the principal quantum number n and $s, p, d, \ldots$ represent the angular momentum quantum number l. The term-diagram for a hydrogen atom is shown in Figure 1.1(a).

Coulomb Interaction between Electrons. The repulsive Coulomb interaction between electrons is given by

$$\hat{V}_{\rm c} = \sum_{i<j} V_{\rm ee}(\mathbf{r}_i - \mathbf{r}_j), \tag{1.3}$$

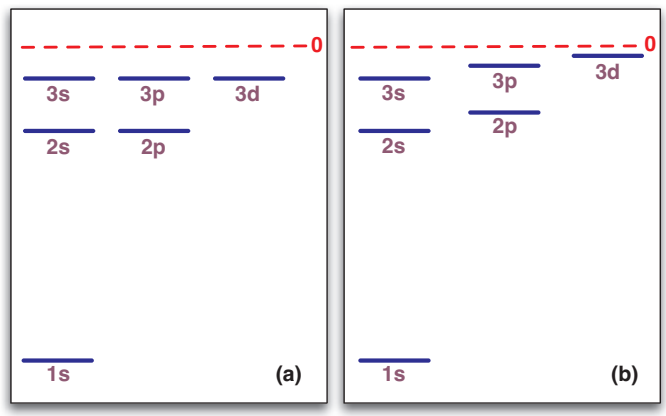

Figure 1.1 Schematic of the term-diagram: (a) the hydrogen atom without screening effect and (b) an alkali-metal atom with screening effect. A color version of this figure can be found in the resources tab for this book at cambridge.org/zhai.

https://doi.org/10.1017/9781108595216.002 Published online by Cambridge University Press

where $V_{ee}(\mathbf{r}) = \kappa/r$. Here we discuss a couple of physical consequences of this term. First, the inner electrons of the fully filled levels screen the positive Ze charge of the nucleus, and thus, the valence electron experiences a reduced Coulomb potential. When the electronic orbit of the outermost electron is far from the nucleus, approximately, it experiences a fully screened field of all the rest of the $Z-1$ electrons. That is to say, for large enough r, the effective attraction between the electron and the nucleus becomes a Coulomb potential with effective charge unity, that is, $-\kappa/r$. The closer this electron approaches toward the nucleus, the more it experiences the unscreened nuclear potential with charge Ze. The attraction between the electron and the nucleus recovers $-Z\kappa/r$ for sufficiently small r. Therefore the effective potential seen by the valance electron is no longer proportional to $1/r$, and hence, the enlarged $SO(4)$ symmetry no longer exists. Consequently, the eigenstates with the same n but different l are no longer degenerate, and the energy level becomes

$$E = -\frac{m^* Z^2 \kappa^2}{2\hbar^2 (n - \delta(n,l))^2}, \tag{1.4}$$

where $\delta(n,l)$ is a function depending on n and l and is also called the "quantum defect" [157]. The term-diagram with the screening effect is schematized in Figure 1.1(b). Normally, the energy level with larger l becomes higher. This energy splitting is also of the order of electron volts, because it also originates from the Coulomb interaction.

Second, let us consider two electrons in two orbits, say, $\psi_1(\mathbf{r})$ and $\psi_2(\mathbf{r})$. Because the total wave function of two electrons has to be antisymmetric, and if these two electrons form a spin singlet, the wave function in the spin space is antisymmetric, and their spatial wave function has to be symmetric, that is, $\psi_1(\mathbf{r}_1)\psi_2(\mathbf{r}_2) + \psi_1(\mathbf{r}_2)\psi_2(\mathbf{r}_1)$. If these two electrons form a spin triplet, the wave function in the spin space is symmetric, and their spatial wave function should be antisymmetric, that is, $\psi_1(\mathbf{r}_1)\psi_2(\mathbf{r}_2) - \psi_1(\mathbf{r}_2)\psi_2(\mathbf{r}_1)$. In the latter case, the wave function vanishes when two electrons come close enough, which reduces the repulsive interaction energy. Thus, the energies of the triplet states are lower than the energy of the singlet state. In other words, the Coulomb repulsion favors the total spin S of electrons to be maximized. This argument can be generalized to cases with more than two electrons and to cases with more than two quantum states, which gives the early day explanation of the first Hund's rule.[1] Also, for a given S, the short-range repulsion is minimized when the total angular momentum L is maximized, which gives the second Hund's rule. The characteristic energy scale of the Hund's rules is also of the order of electron volts.

The Spin-Orbit and Hyperfine Couplings. The Hamiltonian for the spin-orbit coupling is given by

$$\hat{H}_{so} = \sum_i \alpha_f^i \hat{\mathbf{S}}_i \cdot \hat{\mathbf{L}}_i, \tag{1.5}$$

[1] There are more advanced discussions of the origin of the first Hund's rule in later quantum chemistry calculations that we will not discuss in detail here.

https://doi.org/10.1017/9781108595216.002 Published online by Cambridge University Press

and it describes the coupling between the electronic spin $\hat{\mathbf{S}}_i$ and its orbital angular momentum $\hat{\mathbf{L}}_i$ with strength α_{f}^{i} [2], giving rise to the fine structure. The origin of the spin-orbit coupling can be intuitively understood as follows. Sitting in the rest frame of an electron, the nucleus moves around the electron. Because the nucleus is charged, the circulating motion of the nucleus gives rise to an electric current, and the strength of the current is proportional to the angular momentum of the relative motion between the electron and the nucleus. The circulating current further induces a magnetic field, which acts on the spin of electrons. This leads to the spin-orbit coupling given by Eq. 1.5.

As one can see from this picture, because this process involves the magnetic effect induced by the electric current, it is naturally weaker than the Coulomb interaction, because the latter is purely electronic. In fact, the characteristic energy scale of the spin-orbit coupling is typically of the order of 10^{-3}eV ($\sim 10^{11}$Hz), and in many cases it is much weaker than the Hund's rule coupling originating from the Coulomb interaction. Originally, this spin-orbit coupling is between the spin and orbital angular momentum of each individual electron; however, because the Hund's rule coupling locks the electron spins of all valance electrons to an eigenstate of the total electron spin $\hat{\mathbf{S}}$, and locks the angular momentum of all valance electrons to an eigenstate of the total angular momentum $\hat{\mathbf{L}}$, it is more convenient to express the leading order effect of the spin-orbit coupling in terms of $\hat{\mathbf{S}}$ and $\hat{\mathbf{L}}$ as $\alpha_{\mathrm{f}}\hat{\mathbf{S}}\cdot\hat{\mathbf{L}}+\cdots$. Here the first term represents the coupling between $\hat{\mathbf{S}}$ and $\hat{\mathbf{L}}$ with strength α_{f}, which is called the LS coupling. The residual terms represented by $\cdots$ denote the difference between the actual coupling (Eq. 1.5) and the LS coupling term. Because S and L are not really good quantum numbers for Eq. 1.5, these residual terms compete with the Hund's rule and can change the quantum number S and L. Nevertheless, $\hat{\mathbf{J}}=\hat{\mathbf{S}}+\hat{\mathbf{L}}=\sum_i\hat{\mathbf{J}}_i$ still commutes with this coupling.

The hyperfine interaction couples the electronic degrees of freedom $\hat{\mathbf{S}}$ and $\hat{\mathbf{L}}$ to the nucleus spin $\hat{\mathbf{I}}$. In general, $\hat{\mathbf{S}}$ and $\hat{\mathbf{L}}$ couple to $\hat{\mathbf{I}}$ differently. Nevertheless, the characteristic energy scale for the hyperfine coupling is of the order of 10^{-6}eV ($\sim 10^{8}$–10^{9}Hz), which is much smaller compared with the spin-orbit coupling. This is because the nuclear magneton is much smaller than the Bohr magneton. Since the LS coupling already locks $\hat{\mathbf{S}}$ and $\hat{\mathbf{L}}$ to an eigenstate of $\hat{\mathbf{J}}$, we express the leading order effect of the hyperfine coupling in terms of $\hat{\mathbf{J}}$ and $\hat{\mathbf{I}}$ as $\alpha_{\mathrm{hf}}\hat{\mathbf{J}}\cdot\hat{\mathbf{I}}+\cdots$, where α_{hf} is the strength of this coupling. This gives rise to the hyperfine structure. Only with the first term, J is still a good quantum number, but the residual term represented by $\cdots$ can change the quantum number J, which is due to $\hat{\mathbf{S}}$ and $\hat{\mathbf{L}}$ coupled to $\hat{\mathbf{I}}$ differently.

Zoo of Ultracold Atoms. So far, three classes of atoms have been cooled to quantum degeneracy in cold atom experiments. They are (1) alkali-metal atoms, including hydrogen (H), lithium (Li), sodium (Na), potassium (K), rubidium (Rb), and cesium (Cs); (2) alkaline-earth-metal (-like) atoms, including strontium (Sr), calcium (Ca), and ytterbium (Yb). In the periodic table, ytterbium does not belong to the alkaline-earth-metals, but its outer electronic structure is the same as alkaline-earth-metal atoms; and (3) atoms with large electronic magnetic moments, which are called "magnetic atoms" here. These include chromium (Cr), dysprosium (Dy), and erbium (Er). We also anticipate that more atomic

[2] In general, α_{f}^{i} should also depend on spatial position. Here we ignore this dependence for simplicity.

https://doi.org/10.1017/9781108595216.002 Published online by Cambridge University Press

Table 1.1 The electronic structure and the nuclear spin of the alkali-metal atoms used in current experiments

Atom	Valance electron	Label $^{2S+1}L_J$	Nuclear spin I
Li	$2s^1$	$^2S_{\frac{1}{2}}$	^{7}Li ($I = 3/2$, B); ^{6}Li ($I = 1$, F)
Na	$3s^1$	$^2S_{\frac{1}{2}}$	^{23}Na ($I = 3/2$, B)
K	$4s^1$	$^2S_{\frac{1}{2}}$	^{40}K ($I = 4$, F); ^{39}K ($I = 3/2$, B); ^{41}K ($I = 3/2$, B)
Rb	$5s^1$	$^2S_{\frac{1}{2}}$	^{85}Rb ($I = 5/2$, B); ^{87}Rb ($I = 3/2$, B)
Cs	$6s^1$	$^2S_{\frac{1}{2}}$	^{133}Cs ($I = 7/2$, B)

Note: F denotes fermion, and B denotes boson. Here the symbol $^{2S+1}L_J$ labels the electronic structure of each atom.

species can be cooled to quantum degeneracy in the future. Here we will discuss the electronic structure and the spin structure at zero magnetic field of these three classes based on the aforementioned terms.

Alkali-Metal Atoms. So far, all atomic species in Table 1.1 have been cooled to quantum degeneracy, among which ^{87}Rb and ^{23}Na are the most-studied ultracold bosonic isotopes and ^{40}K and ^{6}Li are the most-studied fermionic isotopes. Following are a few key points about this class of atoms:

- In the ground state, since there is only one electron in the s-orbital, $S = 1/2$, $L = 0$, and $J = 1/2$. The ground state is always labeled by $^2S_{1/2}$. There is no spin-orbit coupling in the ground state, and the atomic spin structure is determined by the hyperfine coupling. The hyperfine spin is defined as $\hat{\mathbf{F}} = \hat{\mathbf{I}} + \hat{\mathbf{J}}$, and F is a good quantum number for an alkali-metal atom at the zero magnetic field. For instance, for ^{87}Rb, $I = 3/2$, so the total F can be either 1 or 2. At zero magnetic field, the energy splitting between $F = 1$ states and $F = 2$ states is a few times 10^9Hz.
- For the first excited state, the valance electron is the p-orbital, and thus $L = 1$. Due to the LS coupling, the total J can be either $1/2$ or $3/2$. Thus the excited states are split into $^2P_{\frac{3}{2}}$ and $^2P_{\frac{1}{2}}$, as shown in Figure 1.2(a). Historically, this splitting was discovered in the absorption spectra of lights due to sodium atoms, and they are named as D_1 and D_2 lines. Using sodium as an example, this fine splitting is 2.1×10^{-3}eV ($\simeq 5 \times 10^{11}$Hz), and the splitting between the ground state $^2S_{\frac{1}{2}}$ and these two states is about 2.1eV ($\simeq 5 \times 10^{14}$Hz). Because the fine-structure splitting is much smaller compared with the excitation energy, normally both $^2P_{\frac{3}{2}}$ and $^2P_{\frac{1}{2}}$ should participate in the optical transition, which are key processes for trapping and manipulating alkali-metal atoms, as we shall discuss in Section 1.3 in detail. In addition, $^2P_{\frac{3}{2}}$ and $^2P_{\frac{1}{2}}$ are further split by the hyperfine coupling, and the hyperfine splitting is even smaller compared with the fine-structure splitting.

Alkaline-Earth-Metal (-Like) Atoms. Table 1.2 contains the alkaline-earth-metal atoms (Ca and Sr) and alkaline-earth-metal-like atom (Yb) that have been cooled to quantum

https://doi.org/10.1017/9781108595216.002 Published online by Cambridge University Press

Table 1.2 The electronic structure and the nuclear spin of alkaline-earth-metal (-like) atoms used in current experiments

Atom	Valance electron	Label $^{2S+1}L_J$	Nuclear spin I
Yb	$4f^{14}6s^2$	$^1S_0$	^{174}Yb ($I = 0$, B); ^{171}Yb ($I = 1/2$, F); ^{173}Yb ($I = 5/2$, F)
Ca	$4s^2$	$^1S_0$	^{40}Ca ($I = 0$, B)
Sr	$5s^2$	$^1S_0$	^{84}Sr ($I = 0$,B); ^{87}Sr ($I = 9/2$, F)

Note: F denotes fermion, and B denotes boson.

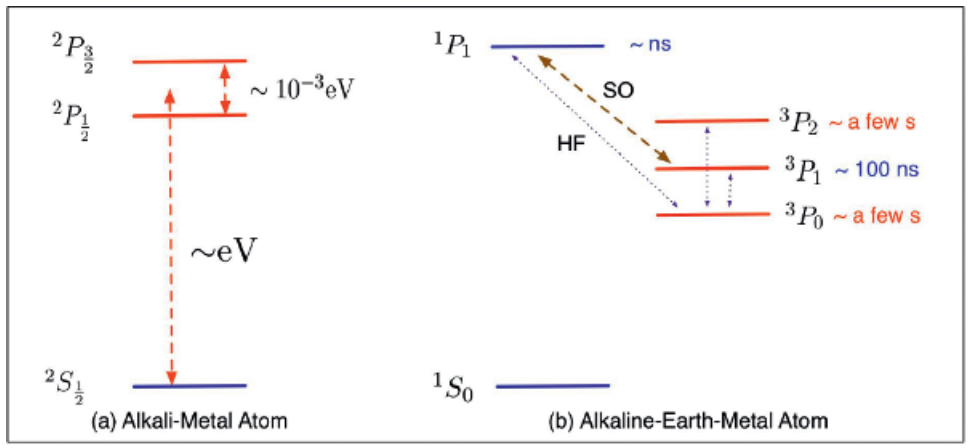

Figure 1.2 Schematic of the electronic structure: (a) an alkali-metal atom and (b) an alkaline-earth-metal atom. The dashed line in (a) denotes the excitation energy, and the dashed lines in (b) denote that these states are coupled either by the spin-orbit coupling (SO) or by the hyperfine coupling (HF) process. A color version of this figure can be found in the resources tab for this book at cambridge.org/zhai.

degeneracy. Alkaline-earth-metal atoms have several unique properties compared with the alkali-metal atoms:

- For the ground state, two electrons occupy the s-orbital, and therefore, the total electron spin $S = 0$ and the angular momentum $L = 0$. All bosonic isotopes of alkaline-earth-metal atoms have zero nuclear spin, and the fermionic isotopes have nonzero nuclear spin I, which can be very large. However, because of $J = 0$, and consequently, the absence of the hyperfine coupling, the nuclear spin is decoupled from the electronic spin degree of freedom. Therefore, the nuclear spin nearly does not participate in two-body interactions, and the interaction possesses an $SU(N)$ symmetry with large-N [193]. We will discuss this in Section 2.3.
- For the first excited states, one electron still occupies the s-orbital, but the other electron is excited to the p-orbital. Thus, these states have $L = 1$. The electronic structure of these excited states is shown in Figure 1.2(b). First of all, because of the Hund's rule, the Coulomb energies for the $S = 1$ states (^3P_J) are lower than that for the $S = 0$ state

https://doi.org/10.1017/9781108595216.002 Published online by Cambridge University Press

($^1P_1$). Second, due to the LS coupling, all states within the $S = 1$ manifold split into $J = 0$, 1, and 2, denoted by $^3P_0$, $^3P_1$,$^3P_2$, respectively.

- As we will see in Section 1.3, because the optical transition is dominated by the dipole transition, and the dipole transition does not change the electronic spin quantum number S, the direct coupling between these excited states with $S = 1$ (^3P_J) and the ground state with $S = 0$ is forbidden because of different quantum number S. That is to say, at the leading order, the dipole transition can only couple the ground state to the $S = 0$ excited state ($^1P_1$) and cannot couple the ground state to the $S = 1$ manifold (^3P_J).
- As we have mentioned above, the spin-orbit coupling term does not conserve the quantum number S and L, and it can mix two states as long as they have the same J. Thus, among the three states with $S = 1$, $^3P_1$ states can be coupled to $^1P_1$ states by the spin-orbit coupling. Through this coupling, there exists a small but finite dipole transition matrix element between the $^3P_1$ states and the ground state. This gives rise to a lifetime for $^3P_1$ states of about a few hundred nanoseconds. And for $^3P_0$ and $^3P_2$, because their quantum numbers J are different from that of $^1P_1$, they cannot be coupled to $^1P_1$ by the spin-orbit coupling term.
- For fermionic isotopes, the coupling between $^3P_0$ or $^3P_2$ and $^1P_1$ can be induced by the hyperfine coupling. As we have discussed above, after including the hyperfine coupling, J is also not a good quantum number. However, the coupling mediated by the hyperfine coupling is much weaker, and hence, the lifetimes of $^3P_0$ and $^3P_2$ states are much longer than for $^3P_1$ states, and the lifetime can be many seconds. These long-lived electronic excited states can be used as an important tool for precision measurement. On one hand, the spontaneous emission rates of these states are so small, and on the other hand, the coupling is not completely forbidden because of these residual couplings. Taking advantage of these properties, the transition between $^3P_0$ and $^1S_0$ induced by laser coupling can be used for the purpose of realizing the atomic optical clock. Therefore, these states are also called the "clock state." The atomic optical clock has reached an accuracy of 10^{-19}s nowadays, and it is the most accurate clock we have now [25]. If one were to start to run such a clock from the beginning of the universe until now, this clock would be expected neither to gain nor to lose even one second. Such a clock can now be used to test fundamental physics [92].
- For bosonic isotopes, due to the absence of the nuclear spin, there is absolutely no one-photon dipole transition for $^3P_0$ and $^3P_2$. In this case, the coupling to ground state has to be induced by higher-order processes. The lifetime of these two states can be many years long, and for all practical purposes, these states can be viewed as not decayed.

Magnetic Atoms. Table 1.3 contains three atoms whose total angular momentum of electron J is very large. For chromium, five d-orbitals and one s-orbital are all half-filled, and thus all six electrons are spin polarized because of the first Hund's rule, which gives $S = 3$ and $L = 0$. Dysprosium and erbium are open-shell lanthanide atoms. For dysprosium, 7 f-orbitals are filled by 10 electrons, and thus there are 4 unpaired electrons. Because of the first Hund's rule, these four unpaired electrons are spin polarized, which gives rise to a total electronic spin $S = 2$. And because of the second Hund's rule, these four unpaired electrons give maximized angular momentum $L = 6$. Similarly, for erbium, 7 f-orbitals

https://doi.org/10.1017/9781108595216.002 Published online by Cambridge University Press

Table 1.3 The atomic structure of high-spin magnetic atoms like Cr and lanthanide Dy and Er

Atom	Valance electron	Label $^{2S+1}L_J$	Nuclear spin I
Cr	$3d^5 4s^1$	$^7S_3$	^{52}Cr ($I = 0$, B); ^{53}Cr ($I = 3/2$, F)
Dy	$4f^{10}6s^2$	$^5I_8$	^{162}Dy ($I = 0$, B); ^{163}Dy ($I = 5/2$, F)
Er	$4f^{12}6s^2$	$^3H_6$	^{168}Er ($I = 0$,B)

Note: F denotes fermion, and B denotes boson.

are filled by 12 electrons, and thus there are 2 unpaired electrons, which gives $S = 1$ and a maximized angular momentum $L = 5$. Furthermore, it turns out that for both Dy and Er, the spin-orbit coupling favors a maximum J, that is, $J = 8$ for dysprosium and $J = 6$ for erbium. The atomic structures of these atoms also have strong effects on the interaction between these atoms:

- In the presence of a finite magnetic field, **J** can be easily polarized, which results in a magnetic moment $d = 6\mu_B$ for chromium, $d = 10\mu_B$ for dysprosium, and $d = 7\mu_B$ for erbium. Therefore, the magnetic moment is about one order of magnitude larger than that of the alkali-metal atoms, and hence the magnetic dipole interaction between two atoms is two orders of magnitude larger.
- In the presence of a finite magnetic field, because the angular momentum L is nonzero for dysprosium and erbium, the electron cloud is anisotropic, so that the short-range Van der Waals potential is also anisotropic. This effect does not exist in chromium, whose angular momentum is zero.
- In the limit of a vanishing magnetic field, **J** becomes depolarized, and the spin rotational symmetry is restored. These atoms exhibit the aspects of high-spin particles, and their interactions depend on spin, as we will discuss in Section 4.3.

1.2 Magnetic Structure

Now we consider the effect of a static magnetic field on the atomic structure. Because electrons are charged, in principle, the electron motion inside an atom can also be affected by the presence of magnetic field. However, this effect is too small compared with the Coulomb interaction, such that we can safely ignore the change of electron orbital due to the magnetic field. We only focus on the Zeeman effect acting on the electron spin **S**, orbital angular momentum **L**, and nuclear spin **I**. The energy scale of the Zeeman splitting is comparable with the hyperfine splitting for a typical magnetic field of hundreds of Gauss in the laboratory.

Hence, here we consider an atom as a point neural particle carrying **S**, **L**, and **I**. Now let us focus on the ground state of alkali-metal atoms. For example, for ^{87}Rb atoms with $S = 1/2$, $L = 0$, and $I = 3/2$, the ground state spin structure is determined by

$$\hat{H}_s = B(\mu_B g_S \hat{S}_z + \mu_N g_I \hat{I}_z) + \alpha_{hf}\, \hat{\mathbf{J}} \cdot \hat{\mathbf{I}}, \tag{1.6}$$

https://doi.org/10.1017/9781108595216.002 Published online by Cambridge University Press

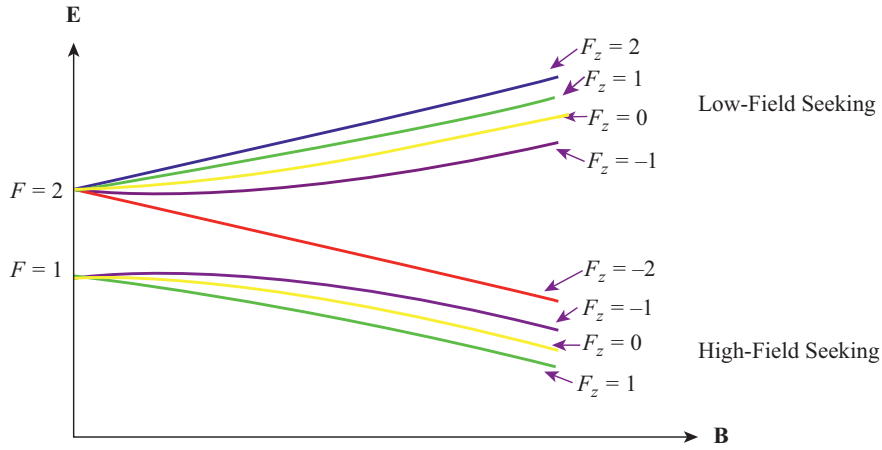

Figure 1.3 Schematic of the Zeeman energy structure. Here we consider the electronic ground state of a ^{87}Rb atom with $J = 1/2$ and $I = 3/2$. F_z labels the good quantum number of each state. A color version of this figure can be found in the resources tab for this book at cambridge.org/zhai.

where μ_B and μ_N are the Bohr magneton and the nuclear magneton, respectively, and $\mu_N \ll \mu_B$. g_S and g_I are the Landé g-factors. Here we first consider the situation that the magnetic field is spatially uniform and its direction is chosen as the $\hat{z}$ direction. For this Hamiltonian, F_z is a good quantum number, and its spectrum can be solved exactly. Here we analyze the behavior in the small B and large B regimes, respectively. By smoothly connecting the small B and large B regimes, one naturally obtains the qualitative feature for the energy diagram, as shown in Figure 1.3

- In the small B-field regime, when $B\mu_B g_s \ll \alpha_{hf}$, the hyperfine coupling dominates. The hyperfine coupling splits the energy between states with $F = 1$ and the states with $F = 2$. Within the three $F = 1$ states, or the five $F = 2$ states, the Zeeman field simply creates a linear Zeeman energy and a quadratic Zeeman energy proportional to F_z and F_z^2, respectively. The reason that there exists a quadratic Zeeman effect is precisely because the hyperfine spin contains both electronic spin and nuclear spin components, and they couple to the external magnetic moment differently.
- In the large B-field regime, when $B\mu_B g_S \gg \alpha_{hf}$, the Zeeman energy of electron spin dominates. The energies of four states with $S_z \approx -1/2$ decrease as B increases, and the energies of the other four states with $S_z \approx 1/2$ increase as B increases.

Magnetic Trap. In the presence of a magnetic field, the energies of some spin states increase with an increasing magnetic field strength. That is to say, if an atom is prepared in such a state, it can be trapped in the regime where the magnetic field strength has a local minimum. Atoms in these states are called the "low-field seeking" atoms. The energies of some other states decrease with an increasing magnetic field strength. These states can be trapped in the regime where the magnetic field strength has a local maximum. Atoms in these states are called the "high-field seeking" atoms. This is the basic idea of the magnetic

https://doi.org/10.1017/9781108595216.002 Published online by Cambridge University Press

trapping. It is not difficult to show that, due to the constraint from the Maxwell equations, the magnetic field cannot have a local maximum if there is no electronic current inside a vacuum chamber. It can also be shown that the magnetic field cannot point to the same direction in order to create a local minimum of magnetic field strength in space. Thus, the natural idea is to trap the "low-field seeking" atoms by a minimum of the magnetic field strength, using a spatially varying magnetic field texture. For instance, a so-called quadrupole trap has a magnetic field configuration $\mathbf{B} = B_0(x, y, -2z)$, where $\mathbf{r} = (x, y, z)$ is the spatial coordinate and the magnetic field strength has a minimum at $\mathbf{r} = 0$.

Emergent Synthetic Gauge Field. Above we have studied the Zeeman energy level of an atom in a uniform magnetic field, which results in the idea of trapping atoms near a minimum of the magnetic field strength. On the other hand, we have also noticed that the magnetic field cannot point to the same direction in order to have a local minimum of its strength. Thus, to fill the gap, we have to consider the motion of an atom in a spatially varying magnetic field configuration $\mathbf{B}(\mathbf{r})$. Let us consider the Schrödinger equation for the motion of an atom as

$$i\hbar\frac{\partial\psi}{\partial t} = \left(-\frac{\hbar^2}{2m}\nabla^2 + \hat{H}_{\rm s}(\mathbf{r})\right)\psi, \tag{1.7}$$

where

$$\hat{H}_{\rm s}(\mathbf{r}) = \mu_{\rm B} g_{\rm S}\mathbf{B}(\mathbf{r})\cdot\hat{\mathbf{S}} + \mu_{\rm N} g_{\rm I}\mathbf{B}(\mathbf{r})\cdot\hat{\mathbf{I}} + \alpha_{\rm hf}\hat{\mathbf{J}}\cdot\hat{\mathbf{I}}. \tag{1.8}$$

We introduce a unitary matrix $\mathcal{U}(\mathbf{r})$ to diagonalize $\hat{H}_{\rm s}(\mathbf{r})$ as $\Lambda(\mathbf{r}) = \mathcal{U}^\dagger(\mathbf{r})\hat{H}_{\rm s}(\mathbf{r})\mathcal{U}(\mathbf{r})$ for every $\mathbf{r}$. For each $\mathbf{r}$, we can always choose a local coordinate such that the magnetic field direction is taken as local $\hat{z}$ direction, therefore, $\Lambda(\mathbf{r})$ has the same energy level as shown in Figure 1.3 for the Hamiltonian Eq. 1.6 that only depends on the strength $|\mathbf{B}(\mathbf{r})|$.

Denoting $\tilde{\psi} = \mathcal{U}^\dagger(\mathbf{r})\psi$, the Schrödinger equation for $\tilde{\psi}$ can be written into the adiabatic spin bases as

$$i\hbar\frac{\partial\tilde{\psi}}{\partial t} = \left(\frac{1}{2m}(-i\hbar\nabla - \mathbf{A})^2 + \Lambda(\,\mathbf{r})\right)\tilde{\psi}, \tag{1.9}$$

where $\mathbf{A}(\mathbf{r}) = i\hbar\mathcal{U}^\dagger(\mathbf{r})(\nabla\mathcal{U}(\mathbf{r}))$. Here we have used

$$\mathcal{U}^\dagger(-i\hbar\nabla)\mathcal{U} = -i\hbar\nabla - i\hbar\mathcal{U}^\dagger(\mathbf{r})(\nabla\mathcal{U}(\mathbf{r})). \tag{1.10}$$

Notice that $\mathcal{U}^\dagger(\mathbf{r})\mathcal{U}(\mathbf{r}) = 1$, which means

$$\mathcal{U}^\dagger(\mathbf{r})(\nabla\mathcal{U}(\mathbf{r})) + (\nabla\mathcal{U}^\dagger(\mathbf{r}))\mathcal{U}(\mathbf{r}) = 0, \tag{1.11}$$

and $\mathcal{U}^\dagger(\mathbf{r})(\nabla\mathcal{U}(\mathbf{r}))$ is purely imaginary. Thus $\mathbf{A}$ is a real field. Eq. 1.9 takes the same form as the Schrödinger equation for the motion of a particle in an external gauge field [73]. In cold atom literatures, this emergent gauge field $\mathbf{A}$ is called the "synthetic gauge field."

Gauge fields are classified as abelian and non-abelian. For abelian ones, different components of the gauge field commute with each other, for instance, when $\mathbf{A}$ is a number. For non-abelian ones, different components of the gauge field do not commute with each other. Here, in general, $\mathbf{A}$ is a matrix, and different spatial components of $\mathbf{A}$ do not commute with each other, which represents a non-abelian gauge field. The off-diagonal component

https://doi.org/10.1017/9781108595216.002 Published online by Cambridge University Press

of $\mathbf{A}$ gives rise to the transition between different spin eigenstates in local coordinates. If these off-diagonal components are too small compared with the difference between the diagonal components of $\Lambda(\mathbf{r})$, the transition effect becomes negligible, and one can safely assume that the atoms always stay in the same adiabatic spin eigenstate. It is usually the case when the magnetic field strength is large and the spatial variation is small. Using the adiabatic approximation, an atom in this adiabatic spin state can effectively be viewed as a spinless particle, which experiences a potential only depending on the strength $|\mathbf{B}(\mathbf{r})|$. This manifests the magnetic trapping as discussed above. The only modification is the presence of the diagonal component of the gauge field $\mathbf{A}$, say, denoted by A_{ii}, corresponding to the adiabatic spin eigenstate labeled by i. This gives rise to an abelian gauge field. This abelian gauge field has a physical effect when it leads to a nonzero synthetic magnetic field $\mathbf{B}_{\text{syn}}$, given by $\mathbf{B}_{\text{syn}} = \nabla \times \mathbf{A}_{ii}(\mathbf{r})$.

The discussion above says that the motion of a neural atom with spin in a spatially varying magnetic field $\mathbf{B}(\mathbf{r})$ is equivalent to the motion of a spinless charged particle in a synthetic magnetic field $\mathbf{B}_{\text{syn}}$. This synthetic magnetic field $\mathbf{B}_{\text{syn}}$ should not be confused with the real magnetic field $\mathbf{B}$. The real magnetic field $\mathbf{B}$ only acts on the spin degree of freedom of an atom and does not couple to its motion because atoms are neutral. However, the synthetic gauge field only acts on the motion of the particle. This equivalence is emergent from the Berry phase effect, and the basic idea is illustrated in Figure 1.4. Let us consider a neutral atom with spin moving in a spatially varying magnetic field. Following the adiabatic approximation, when an atom moves, its spin direction is always aligned with the local magnetic field direction. Therefore, when the atom follows a closed trajectory in space, its wave function acquires an extra phase that is proportional to the solid angle expanded by the spin direction along the trajectory. On the other hand, for a charged particle moving in a magnetic field, due to the Aharonov–Bohm effect, it also requires a phase for any closed trajectory which is proportional to the total flux enclosed by the trajectory. If these two

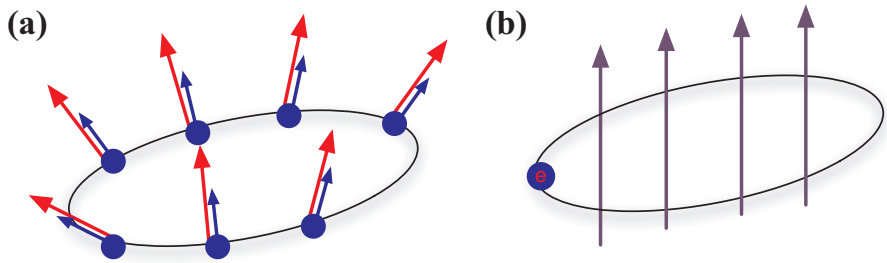

Figure 1.4 Emergence of synthetic gauge field. (a) A neutral and spinful atom (represented by the filled circles) moves in a magnetic field with spatially varying magnetic field directions (represented by longer arrows), and its spin direction (represented by arrows attached to the filled circles) always follows the local magnetic field direction. (b) A charged spinless particle moves in a magnetic field (represented by the vertical arrows). These two motions are equivalent when (i) the adiabatic approximation for case (a) is valid and (ii) the phases accumulated along any trajectory are always equal between cases (a) and (b). A color version of this figure can be found in the resources tab for this book at cambridge.org/zhai.

https://doi.org/10.1017/9781108595216.002 Published online by Cambridge University Press

Box 1.1 Different Kinds of "Magnetic Fields"

It is really important to distinguish these three concepts of the real magnetic field, the light-induced magnetic field, and the synthetic magnetic field. Here we summarize the difference and the relations between these three "magnetic fields." First of all, the former two act on the spin degree of atoms, and the third one acts on the spatial motion of atoms. Second, both the real and the light-induced magnetic fields can polarize spin of atoms in a spatially dependent way, which leads to the synthetic magnetic field. Third, the synthetic magnetic field generated by the light-induced magnetic field can be much stronger than that generated by the real magnetic field. The synthetic gauge field is an active research topic in cold atom physics, and more discussion can be found in Box 7.3.

phases are always equal for any trajectory, then the spatial motion of a neutral spinful atom in a spatially varying magnetic field can be effectively described by a "charged" spinless particle in a synthetic magnetic field. This also tells us that the synthetic magnetic flux generated in this way depends on how fast the magnetic field direction varies in space. However, it is hard for a real magnetic field to vary very rapidly in space. In Section 1.3 we will introduce the vector light shift, which can generate a light-induced Zeeman field for atoms that can vary in the scale of the order of interparticle spacing. By combining these two effects, we can generate a strong synthetic magnetic field. To further clarify these concepts, we summarize different terminology of "magnetic fields" in Table 1.1.

Finally, we should also mention that this adiabatic approximation can break down either when the off-diagonal components of $\mathbf{A}$ become very large due to fast variation of the magnetic field direction or when the energy differences of the diagonal components of $\Lambda(\mathbf{r})$ become quite small. For instance, the latter happens at $\mathbf{r} = 0$ of the quadruple trap, where a few spin states become degenerate. Around the $\mathbf{r} = 0$ regime, the off-diagonal components of $\mathbf{A}$ are always important, which drives transitions between different adiabatic spin states. Therefore, there is significant probability that a "low-field seeking" state can flip into a "high-field seeking" state, which is also known as the "Majorana transition." When the transition takes place, atoms cannot be trapped by the magnetic trap. This is one of the major challenges in achieving a Bose–Einstein condensate in a magnetic trap before 1995. This is actually an effect of the non-abelian gauge field. It is interesting to note that though the synthetic gauge field became a major research subject in cold atom physics after around 2010, its effect already existed even prior to the birth of this field. The JILA group and the MIT group came up with different methods to solve this problem. The JILA group applies an oscillating offset magnetic field to deal with this problem [140]. Treating a time-periodical system requires the Floquet theory, which will also be discussed in Section 7.4.

1.3 Light Shift

In the previous sections, we discussed the structure of a single atom. In this section, we will discuss how a single atom interacts with a laser light.

https://doi.org/10.1017/9781108595216.002 Published online by Cambridge University Press

General Framework. Atoms experience an effective potential in the presence of the laser field. Here we will discuss such potential using the ground state alkali-metal atoms as an example. One can see that the first two leading order contributions to this light-induced potential are the scalar potential and the vector potential, which are known as the scalar light shift and the vector light shift, respectively.

As discussed in Section 1.1, let us consider all states in the ground state ${}^2S_{\frac{1}{2}}$ manifold with the electron angular momentum $L = 0$, and all states in the electronic excited states ${}^2P_{\frac{1}{2}}$ and ${}^2P_{\frac{3}{2}}$ manifolds with $L = 1$. Here, by "manifold," we mean that both electronic and nuclear spin degrees of freedom are included, and each manifold contains multiple spin states. The energy splitting E_{ex} between the ground and the excited manifolds is of the order of the electron volt, which usually lies in the energy window of a visible light field, as shown in Figure 1.5. We denote the detuning $\Delta_{\text{e}} = E_{\text{ex}} - \hbar\omega$, where ω is the laser frequency. Usually, Δ_{e} is comparable to or larger than the fine-structure splitting and is much larger than the hyperfine splitting. Δ_{e} is also much smaller than the detuning of the other electronic excited states, that is to say, all the other electronic excited states are far detuned. With these energy scale considerations, our model is established as follows:

- The contributions from both ${}^2P_{\frac{1}{2}}$ and ${}^2P_{\frac{3}{2}}$ are important and should be treated on equal footing.
- The hyperfine coupling and the Zeeman energy are safely ignored.
- Except for ${}^2S_{\frac{1}{2}}$, ${}^2P_{\frac{1}{2}}$ and ${}^2P_{\frac{3}{2}}$ manifolds, all the other electronic states are not included.

Hence, we write down our model as follows [61]:

$$\hat{H} = \hat{H}_{\text{at}} + \hat{H}_{\text{d}}. \tag{1.12}$$

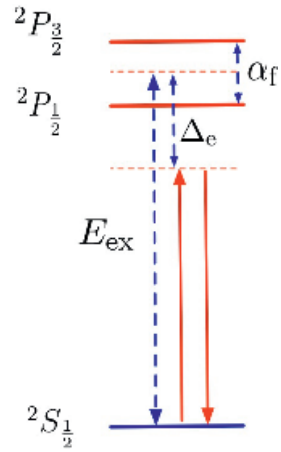

Figure 1.5 Schematic of the level diagram for atom-light interaction. Here we use the alkali-metal atoms as an example. Three relevant energy scales, the excitation energy E_{ex}, the detuning Δ_e, and the fine structure splitting α_{f}, are marked on the diagram. A color version of this figure can be found in the resources tab for this book at cambridge.org/zhai.

https://doi.org/10.1017/9781108595216.002 Published online by Cambridge University Press

$\hat{H}_{\rm at}$ denotes the Hamiltonian for the atom part and it is given by

$$\hat{H}_{\rm at} = E_{\rm ex}\mathcal{P}_{\rm e} + \alpha_{\rm f}\hat{\mathbf{S}}\cdot\hat{\mathbf{L}}. \tag{1.13}$$

Here we define a projection operator $\mathcal{P}_g$ to the ground states manifold with $L = 0$ and a projection operator $\mathcal{P}_e$ to the excited states manifold with $L = 1$. In our model, $\mathcal{P}_g + \mathcal{P}_e = 1$. We have also set the ground state energy as zero energy, and the $\hat{\mathbf{S}}\cdot\hat{\mathbf{L}}$ vanishes when acting on the ground state manifold. It is also important to note that $\hat{H}_{\rm at}$ itself does not provide any coupling between the ground and the excited states.

Here the atom–light interaction refers to the interaction between electrons inside the atom and the electromagnetic field of the laser. Considering a time-dependent electric field applied to electrons, the Hamiltonian can be written as

$$\hat{H} = \sum_{i=1}^{Z} \frac{1}{2m^*}(\hat{\mathbf{p}}_i + e\mathbf{A}(t))^2 + \ldots, \tag{1.14}$$

where $\mathbf{r}_i$ denotes the coordinate of a valance electron in the rest frame of the nucleus, and $\ldots$ represents the Coulomb interactions and other terms discussed in Section 1.1. Typically, the wave length of a laser is much longer than the size of an atom, therefore, on the scale of electronic wave function inside an atom, we can ignore the spatial dependence of $\mathbf{A}$ and only consider its temporal dependence. As we will see below, this leads to the dipolar coupling.

Here, by performing a gauge transformation, we consider $\hat{\mathcal{U}}^\dagger\hat{H}\hat{\mathcal{U}} \to \hat{H}$, and $U^\dagger\psi \to \psi$, and here

$$\hat{\mathcal{U}} = e^{-\sum_i ie\mathbf{A}\cdot\mathbf{r}_i/\hbar}. \tag{1.15}$$

Under this gauge transformation, $\hat{\mathbf{p}}_i + e\mathbf{A}$ changes back to $\hat{\mathbf{p}}_i$ and the kinetic energy returns to the normal $\hat{\mathbf{p}}_i^2/(2m^*)$. However, because this gauge transformation is time dependent, there will be an extra term $i\hbar(\partial_t\hat{\mathcal{U}})^\dagger\hat{\mathcal{U}}$ added into the Hamiltonian, which is given by

$$i\hbar(\partial_t\hat{\mathcal{U}}^\dagger)\hat{\mathcal{U}} = -e\mathbf{r}_i\cdot\frac{\partial\mathbf{A}}{\partial t} = e\mathbf{r}_i\cdot\mathbf{E}, \tag{1.16}$$

where $\mathbf{E}$ is the electric field of the laser given by $\mathbf{E} = -\partial\mathbf{A}/\partial t$. Hence, it results in the dipole coupling $\hat{H}_{\rm d} = \mathbf{d}\cdot\mathbf{E}$, where $\mathbf{d} = \sum_i e\mathbf{r}_i$ is the electron dipole operator, and it gives rise to the transition between the ground and the excited states.

First, we consider a single laser field, and

$$\hat{H}_{\rm d} = \mathbf{d}\cdot\mathbf{E} = \sum_{j=x,y,z} d_j E_j^0\cos(\phi_j - \omega t), \tag{1.17}$$

where $E_j^0\cos(\phi_j - \omega t)$ is the jth component of the electric field and $j = x, y, z$ denotes three spatial components of the laser field. For example, in this notation, for a light linearly polarized along $\hat{x}$, $E_x^0 \neq 0$ and $E_y^0 = E_z^0 = 0$; for a light linearly polarized along the $(\hat{x} + \hat{y})/\sqrt{2}$ direction, $E_x^0 = E_y^0 \neq 0$, $\phi_x = \phi_y$ and $E_z^0 = 0$; and for a light circularly polarized in the xy plane, $E_x^0 = E_y^0 \neq 0$, $\phi_x = \phi_y \pm \pi/2$ and $E_z^0 = 0$.

https://doi.org/10.1017/9781108595216.002 Published online by Cambridge University Press

Here we first simply the Hamiltonian by employing the rotating wave approximation. We first define a unitary transformation as

$$\hat{\mathcal{U}}(t) = e^{-i\omega t\mathcal{P}_e} = (1 - \mathcal{P}_e) + \mathcal{P}_e e^{-i\omega t} = \mathcal{P}_g + \mathcal{P}_e e^{-i\omega t}. \tag{1.18}$$

and apply this unitary transformation to the Hamiltonian. The rotating wave approximation ignores $e^{\pm i2\omega t}$ terms because they are high-frequency oscillating terms. With this approximation, it is straightforward to show that the Hamiltonian is reduced to

$$\hat{H}_{\rm d} = \hat{\mathcal{U}}^\dagger(t)\hat{H}_{\rm d}\hat{\mathcal{U}}(t) \approx \frac{1}{2}\sum_{j=x,y,z}\left(\mathcal{E}_j^*\mathcal{P}_g d_j \mathcal{P}_e + \mathcal{E}_j\mathcal{P}_e d_j\mathcal{P}_g\right), \tag{1.19}$$

where we have also used $\mathcal{P}_g d_j \mathcal{P}_g = \mathcal{P}_e d_j \mathcal{P}_e = 0$ because of the rotational symmetry of the electron wave functions. Here $\mathcal{E}_j$ is defined as $E_j^0 e^{i\phi_j}$. Unlike $\mathbf{E}$, here $\boldsymbol{\mathcal{E}}$ is time-independent, which encodes the phase and amplitude information of the laser field. In this notation, for a light linearly polarized along $\hat{x}$, $\boldsymbol{\mathcal{E}} = E_0\mathbf{e_x}$; for a light linearly polarized along the $(\hat{x}+\hat{y})/\sqrt{2}$ direction, $\boldsymbol{\mathcal{E}} = \frac{E_0}{\sqrt{2}}(\mathbf{e_x}+\mathbf{e_y})$; and for a light circularly polarized in the xy plane, $\boldsymbol{\mathcal{E}} = \frac{E_0}{\sqrt{2}}(\mathbf{e_x} + i\mathbf{e_y})$.

Moreover, a time-dependent term $i\hbar(\partial_t\hat{\mathcal{U}}^\dagger)\hat{\mathcal{U}}$ can be absorbed in $\hat{H}_{\rm at}$ so that $\hat{H}_{\rm at}$ becomes

$$\hat{H}_{\rm at} = \Delta_{\rm e}\mathcal{P}_{\rm e} + \alpha_{\rm f}\hat{\mathbf{S}}\cdot\hat{\mathbf{L}}, \tag{1.20}$$

where $\Delta_e = E_{\rm ex} - \hbar\omega$. $\Delta_e > 0$ is called the red detuning and $\Delta_e < 0$ is called the blue detuning. In this way, we obtain the new $\hat{H}_{\rm at} + \hat{H}_{\rm d}$ as a time-independent effective Hamiltonian. We will revisit such a time periodical problem in Section 7.4 with a general theoretical framework known as the Floquet theory.

This formalism can be straightforwardly generalized to the situations with multiple laser beams. In this case, the electric field consists of contributions from all laser beams, and we write the dipole coupling as

$$\hat{H}_{\rm d} = \mathbf{d}\cdot\mathbf{E} = \sum_{\kappa}\sum_{j=x,y,z} d_j E_{j,\kappa}^0\cos(\phi_{j,\kappa} - \omega_\kappa t), \tag{1.21}$$

where κ labels different laser fields. Here different lasers can have different frequencies, but their difference should be small. That is to say, suppose we denote the average of these frequencies as ω; their difference should be much smaller than ω. Therefore, we can still safely drop all terms with $e^{\pm i(\omega_\kappa+\omega)t}$ and retain all terms with $e^{\pm i(\omega_\kappa-\omega)t}$. After the rotating wave approximation, it is easy to show that Eq. 1.19 still holds, except that the definition of $\mathcal{E}_j$ should be modified as

$$\mathcal{E}_j = \sum_{\kappa} E_{j,\kappa}^0 e^{i\phi_{j,\kappa} - i(\omega_\kappa-\omega)t}. \tag{1.22}$$

Note that if all lasers share the same frequency, $\boldsymbol{\mathcal{E}}$ is time-independent. If there are multiple frequencies, $\boldsymbol{\mathcal{E}}$ is also time-dependent.

The physical meaning of the rotating wave approximation can be understood more clearly when we treat the laser as a quantum field labeled by photon number. Let us now consider an atom in the ground state (denoted by $|g\rangle$) in a laser field with N photons (denoted by $|N\rangle$). In the second quantized form, the $\mathbf{d}\cdot\mathbf{E}$ coupling can either create

https://doi.org/10.1017/9781108595216.002 Published online by Cambridge University Press

a photon or annihilate a photon when it couples an atom from the ground state to the excited state. Thus, we shall consider following two different second-order perturbation processes. Starting from the state $|g\rangle|N\rangle$, the atom can either be first excited to the excited state (denoted by $|e\rangle$) by absorbing a photon, such that the intermediate state is $|e\rangle|N-1\rangle$ with energy Δ_e, and then return to the ground state $|g\rangle|N\rangle$ by emitting a photon. The atom can also be first excited to the excited state by emitting a photon, such that the intermediate state is $|e\rangle|N+1\rangle$ with energy $E_{\rm ex}+\hbar\omega$, and then return to the ground state $|g\rangle|N\rangle$ by absorbing a photon. The second process has a much larger intermediate state energy, and therefore, the probability is considerably smaller. The rotating wave approximation is basically to ignore the second process. With the first process alone, by taking the energy of photons into account, the energy detuning changes from $E_{\rm ex}$ in Eq. 1.13 to Δ_e in Eq. 1.20.

Hereafter we will consider how this second-order process generates an effective potential for atoms in the ground state manifold after eliminating the excited states $|e\rangle|N-1\rangle$. Following the standard perturbation theory, the effective Hamiltonian for atoms in the ground manifold is derived as

$$\hat{H}_{\rm eff}=-\mathcal{P}_g\hat{H}_{\rm d}\mathcal{P}_e\hat{H}_{\rm at}^{-1}\mathcal{P}_e\hat{H}_{\rm d}\mathcal{P}_g=-\frac{1}{4}\sum_{i,\,j=x,y,z}\mathcal{E}_i^*\hat{\mathcal{D}}_{ij}\mathcal{E}_j, \tag{1.23}$$

where $\hat{\mathcal{D}}_{ij}$ is a rank-2 Cartesian tensor operator defined as

$$\hat{\mathcal{D}}_{ij}=\mathcal{P}_g d_i\mathcal{P}_e\hat{H}_{\rm at}^{-1}\mathcal{P}_e d_j\mathcal{P}_g. \tag{1.24}$$

$\hat{\mathcal{D}}_{ij}$ is purely a property of atoms. By using the fact that $\mathcal{P}_g+\mathcal{P}_e=1$ and $\mathcal{P}_g d_i\mathcal{P}_g=0$, $\mathcal{P}_e$ in Eq. 1.24 can be eliminated. Hereinafter we should focus on the properties of $\hat{\mathcal{D}}_{ij}$ in different circumstances.

The Scalar Light Shift. We first consider a special case with $\alpha_{\rm f}=0$; then $\hat{H}_{\rm at}$ is simplified as $\Delta_e\mathcal{P}_e$, and

$$\hat{\mathcal{D}}_{ij}=\frac{1}{\Delta_e}\mathcal{P}_g d_i d_j\mathcal{P}_g. \tag{1.25}$$

Since the ground state has $L=0$, which has the spatial reflection symmetry and rotational symmetry, it is easy to see that $\mathcal{D}_{ij}=0$ if $i\neq j$, and all three $\mathcal{D}_{jj}$ ($j=x,y,z$) are the same. Therefore,

$$\hat{\mathcal{D}}_{ij}=-4u_s\delta_{ij},\quad u_s=-\frac{e^2}{12\Delta_e}\langle g|r^2|g\rangle, \tag{1.26}$$

which gives rise to an effective Hamiltonian

$$\hat{H}_{\rm eff}=u_s\boldsymbol{\mathcal{E}}^2. \tag{1.27}$$

This term acts identically on different spin states of the ground manifold and cannot flip the spin, and this term also does not depend on the polarization of the lasers. This is because the dipole coupling only acts on the orbital degree of freedom of the valance electron, and therefore, in the absence of $\hat{\mathbf{S}}\cdot\hat{\mathbf{L}}$ coupling, the orbital degree of freedom is decoupled from the spin degree of freedom. Hence, this term is called the *scalar light shift*, and u_s is called the atom's scalar ac polarizability. Below we shall discuss some important applications of the scalar light shift.

https://doi.org/10.1017/9781108595216.002 Published online by Cambridge University Press

Trapping Atoms with Laser. The scalar potential only depends on the intensity of the laser. For the red detuning case, $u_s < 0$, atoms will be trapped in the place where the laser intensity is a local maximum. Hence, one can trap atoms with a focused laser beam. This is the basic mechanism of the laser trapping. In this optical trap, all spin states in the ground state manifold will experience identical potentials, and one can fully utilize the spin degree of freedom of atoms, as we will discuss in Section 4.3.

However, there is one complication we should notice. So far what we have considered is the second-order process that the photon absorption is followed by the stimulated emission. In fact, there is another process, that is, the photon absorption is followed by the spontaneous emission. The spontaneous emission is what causes the finite lifetime of the excited state and can be described by adding an imaginary part Γ in the excited state energy, where Γ is the line width of the excited states. Hence, this process can be described by adding an imaginary part to the excited state energy in the expression of the ac polarizability. Consequently, u_s acquires an imaginary part as

$$u_s \propto \frac{1}{\Delta_e - i\Gamma} = \frac{\Delta_e}{\Delta_e^2 + \Gamma^2} + i\frac{\Gamma}{\Delta_e^2 + \Gamma^2}. \tag{1.28}$$

For the off-resonant case with $\Delta_e \gg \Gamma$, the real part behaves as $1/\Delta_e$ and the imaginary part behaves as Γ/Δ_e^2. Since the real and imaginary parts have difference power dependence on Δ_e, in the far-detuned regime with $\Delta_e \gg \Gamma$, the imaginary part can be strongly suppressed compared with the real part. Since the real part provides the trapping effect, one usually works in this far-detuned regime for laser trapping. The laser trapping was awarded the Nobel Prize in 2018.

Optical Lattice. Now let us consider applying two counterpropagating laser beams, say, along $\hat{x}$. These two lasers have the same frequency and the same polarization; for instance, both are linearly polarized along $\hat{y}$. Suppose both two lasers have the same strength E^0; according to Eq. 1.22, we have

$$\mathcal{E}_y = E^0 e^{ikx} + E^0 e^{-ikx} = 2E^0 \cos(kx). \tag{1.29}$$

The electric field intensity has a spatial periodical modulation due to the interference between two lasers. Hence, the scalar light shift gives rise to a periodic lattice potential $V(x) \propto \cos^2(x)$, which is now well known as the optical lattice. Optical lattices will be the main topic of the last part of this book.

Cooling Atoms with Laser. If Δ_e becomes small, the imaginary part of the scalar potential also becomes important, which means the process with spontaneous emission becomes important. There is an important difference between the process with the stimulated emission and the process with the spontaneous emission. For the former, because it is the same photon that is absorbed and emitted, the momentum transfer is canceled, and atoms do not receive momentum transfer after the entire second-order process. But for the latter, since the photon can go any direction in the spontaneous emission process, on average, the momentum transfer during the emission process is canceled out, and therefore, atoms get kicked by the photons of the laser field during absorbing the photon. Effectively, atoms feel a force proportional to Γ/Δ_e^2 and the momentum of the laser. Now considering two

https://doi.org/10.1017/9781108595216.002 Published online by Cambridge University Press

counterpropagating lasers with same frequency, if an atom is at rest, the force from the left laser cancels with the force from the right laser, because the momentum transfers received from the left and the right lasers are of equal strength and opposite sign. However, if an atom moves toward the right, due to the Doppler effect, Δ_e for two lasers depends on the velocities of the atoms, and they are different. Thus, the force cannot be canceled out, and it can be shown that the net force is always opposite to the velocity of the atom [138]. Thus, this effect slows down the motion of atoms. That is the basic mechanism of the laser cooling, which is one of the most important steps to cool atoms toward the quantum degeneracy. Laser cooling was recognized with the Nobel Prize in 1997.

However, due to various limitations, it is very hard to reach quantum degeneracy of atomic gases directly by laser cooling. Directly reaching quantum degeneracy by laser cooling was first achieved more than 20 years after achieving Bose–Einstein condensation in atomic gases [76, 160]. In most experiments, one needs to perform evaporative cooling after laser cooling. The basic idea of evaporative cooling is quite straightforward. Considering that the trapping potential has a finite depth U_0, atoms with kinetic energy larger than U_0 have a significant chance to escape from the trap. Now let us gradually decrease U_0, thus, more and more atoms with larger kinetic energy escape from the trap, and the average kinetic energy of the remaining atoms decreases. Therefore, the temperature of the remaining atomic gas decreases. However, we should notice that the evaporative cooling pays the price of losing atoms in order to lower the temperature. When losing atoms, the degenerate temperature also decreases. Therefore, the efficiency of the evaporative cooling becomes crucial. That is to say, lowering the temperature has to be faster than lowering the degenerate temperature; otherwise, the system can never reach quantum degeneracy. The efficiency of evaporative cooling certainly depends on how to lower the trap depth U_0 as a function of time t, and controlling this dynamical process is the key challenge to reaching quantum degeneracy through evaporative cooling.

Vector Light Shift. Now let us consider the situation with finite $\hat{\mathbf{S}} \cdot \hat{\mathbf{L}}$ coupling. As we discussed above, fine structure splitting α_{f} can be comparable to detuning Δ_{e}. Here, just to simplify the calculation, we consider the situation $\alpha_{\mathrm{f}}/\Delta_{\mathrm{e}} \ll 1$, and the main conclusion does not change if $\alpha_{\mathrm{f}} \sim \Delta_{\mathrm{e}}$. When $\alpha_{\mathrm{f}}/\Delta_{\mathrm{e}} \ll 1$, we can expand $\hat{H}_{\mathrm{at}}^{-1}$ to the leading order of $\alpha_{\mathrm{f}}/\Delta_{\mathrm{e}}$, and we obtain

$$\hat{H}_{\mathrm{at}}^{-1} = \left(\frac{1}{\Delta_e} - \frac{\alpha_{\mathrm{f}}}{\Delta_e^2}\hat{\mathbf{S}} \cdot \hat{\mathbf{L}}\right)\mathcal{P}_e, \tag{1.30}$$

and therefore,

$$\hat{\mathcal{D}}_{ij} = \mathcal{P}_g d_i \frac{1}{\Delta_e} d_j \mathcal{P}_g - \frac{\alpha_{\mathrm{f}}}{\Delta_e^2}\mathcal{P}_g d_i (\hat{\mathbf{S}} \cdot \hat{\mathbf{L}}) d_j \mathcal{P}_g. \tag{1.31}$$

As shown above, the first term gives the scalar part. And for the second term, one has

$$\mathcal{P}_g d_i (\hat{\mathbf{S}} \cdot \hat{\mathbf{L}}) d_j \mathcal{P}_g = \mathcal{P}_g (\hat{\mathbf{S}} \cdot \hat{\mathbf{L}}) d_i d_j \mathcal{P}_g - \mathcal{P}_g [(\hat{\mathbf{S}} \cdot \hat{\mathbf{L}}), d_i] d_j \mathcal{P}_g \tag{1.32}$$

$$= -i\hbar \epsilon_{lim} S_l \mathcal{P}_g d_m d_j \mathcal{P}_g, \tag{1.33}$$

https://doi.org/10.1017/9781108595216.002 Published online by Cambridge University Press

where the first term vanishes because ground state has $\hat{\mathbf{L}}\mathcal{P}_g = 0$, and for the second term, we have used the commutative relation $[\hat{L}_l, \hat{d}_i] = i\hbar\epsilon_{lim}\hat{d}_m$, where ϵ_{jim} is the Levi–Civita symbol. Thus we reach

$$\hat{\mathcal{D}}_{ij} = -4u_s\delta_{ij} + i\frac{\hbar\alpha_f}{\Delta_e}\epsilon_{ijl}S_l(-4u_s) \simeq -4u_s\left(\delta_{ij} + i\frac{\hbar\alpha_f}{\Delta_e}\epsilon_{ijl}S_l\right), \tag{1.34}$$

where the second term will give rise to a vector light shift. In this case, the effective Hamiltonian is given by

$$\hat{H}_{\text{eff}} = -\frac{1}{4}\sum_{i,j=x,y,z}\mathcal{E}_i^*\hat{\mathcal{D}}_{ij}\mathcal{E}_j = u_s|\boldsymbol{\mathcal{E}}|^2 + iu_v(\boldsymbol{\mathcal{E}}^* \times \boldsymbol{\mathcal{E}})\cdot\hat{\mathbf{S}}, \tag{1.35}$$

where $u_v = \hbar\alpha_f u_s/\Delta_e$ is the vector polarizability. The physical meaning of the vector light shift is a Zeeman field $\mathbf{B} = iu_v\boldsymbol{\mathcal{E}}^* \times \boldsymbol{\mathcal{E}}$ acting on the electronic spin degree of freedom of an alkali-metal atom.

Again, because the dipole coupling acts on the orbital degree of freedom, the vector light shift has to reply on the $\hat{\mathbf{S}}\cdot\hat{\mathbf{L}}$ coupling that hybridizes the orbital degree of freedom with the electronic spin degree of freedom. In this case, the $\hat{\mathbf{S}}\cdot\hat{\mathbf{L}}$ exists only in the excited states, and therefore, the vector light shift is smaller than the scalar term by an order of $\hbar\alpha_F/\Delta_e$. Consequently, the vector light shift scales with Δ_e also as $1/\Delta_e^2$. Thus, the vector light shift has the same scaling as the spontaneous emission process. In the discussion of the scalar light shift, we have noticed that, because the scalar light shift and the spontaneous emission scale with Δ_e differently, one can suppress the effect of spontaneous emission compared with the scalar potential by increasing the detuning. However, this no longer works for the vector light shift. Because the vector light shift and the spontaneous emission scale with Δ_e in the same way, one cannot suppress the spontaneous emission process without reducing the strength of the vector light shift. This discussion of atom–light interaction can also be generalized to lanthanide atoms like Dysprosium and Erbium [41]. There, the f-orbital is not fully filled for the ground state, and electric spin and angular momentum are not good quantum numbers for atoms in their ground state. Therefore, the dipole coupling can always act on the electronic spin degree of freedom. Thus, for these lanthanide atoms, the vector light shift scales in the same way as the scalar light shift, and they both scale as $1/\Delta_e$ [41, 24]. Indeed, the vector light shift has been realized in the lanthanide atoms with suppressed spontaneous emission [41, 24].

Light-Induced Zeeman Energy. Below we will discuss a couple of examples as the applications of the vector light shift. If an atom is illuminated in a linearly polarized light, then $\boldsymbol{\mathcal{E}}^* \times \boldsymbol{\mathcal{E}} = 0$, and the vector light shift vanishes. If the light is circularly polarized, for instance, $\boldsymbol{\mathcal{E}} = \frac{E_0}{\sqrt{2}}(\mathbf{e_x} + i\mathbf{e_y})$, then

$$\boldsymbol{\mathcal{E}}^* \times \boldsymbol{\mathcal{E}} = iE_0^2\mathbf{e_z}, \tag{1.36}$$

which gives rise to a light-induced Zeeman energy proportional to $u_v E_0^2 S_z$. This difference between a linear polarized light and a circular polarized light lies between their difference in symmetry. The presence of a linear polarized light does not break the time reversal symmetry, but the presence of a circular polarized light does. Since the presence of a Zeeman

https://doi.org/10.1017/9781108595216.002 Published online by Cambridge University Press

field breaks the time-reversal symmetry, symmetry-wise, it is compatible with the presence of a circular polarized light, but is not compatible with the presence of a linearly polarized light.

Since u_v depends on the fine-structure splitting and detuning, if two different atoms are illuminated in the same circular polarized laser, they will experience different light-induced Zeeman fields. In general, because the spin-orbit coupling is stronger for heavier atoms, the vector light shift is also larger for heavier atoms for a given detuning. One experiment that can demonstrate this effect is the spin exchanging scattering between ^{23}Na and ^{87}Rb atoms [108]. The spin exchanging scattering will be discussed in detail in Section 2.3. Here let us first mention it briefly. Considering the $F = 1$ spin states of both ^{23}Na and ^{87}Rb atoms, each of them has three magnetic states labeled by $|F_z\rangle$. For instance, one of the spin-exchanging scattering processes can take place as

$$|0\rangle_{\mathrm{Na}}|-1\rangle_{\mathrm{Rb}} \leftrightarrow |-1\rangle_{\mathrm{Na}}|0\rangle_{\mathrm{Rb}}. \tag{1.37}$$

This spin-exchanging scattering reaches a resonance at a certain magnetic field when the Zeeman energy difference between the incoming and the outgoing states vanishes, that is,

$$\Delta E = (E_{|0\rangle_{\mathrm{Na}}} + E_{|-1\rangle_{\mathrm{Rb}}}) - (E_{|-1\rangle_{\mathrm{Na}}} + E_{|0\rangle_{\mathrm{Rb}}}) = 0, \tag{1.38}$$

at which the period of the spin-exchanging oscillation reaches a maximum. The Zeeman energy contains a contribution from both the static magnetic field and the light-induced Zeeman field. In the common practical condition [108], given a typical value of the optical trapping laser, the light-induced Zeeman energy for ^{87}Rb is equivalent to applying a magnetic field of $\sim$mG, but the light-induced Zeeman energy for ^{23}Na is only equivalent to applying a magnetic field of $\sim \mu$G, which can be safely ignored. This difference is due to the difference in their fine-structure splitting. Therefore, the magnetic field strength to reach the spin-exchanging resonance is different for different laser intensities. This has been experimentally observed, and the experimental results are shown in Figure 1.6.

Synthetic Spin-Orbit Coupling. Now we consider atoms in a real static magnetic field along $\hat{z}$ that gives rise to a Zeeman energy, assumed to be hF_z for simplicity. In addition, let us consider two counterpropagating Raman beams along $\hat{x}$, with one polarized along $\hat{y}$ and the frequency ω_1 and the other polarized along $\hat{z}$ and the frequency ω_2, as shown in Figure 1.7. The electronic field is given by

$$\mathbf{E} = E_1 e^{ik_0 x + i\omega_1 t}\mathbf{e_y} + E_2 e^{-ik_0 x + i\omega_2 t}\mathbf{e_z}. \tag{1.39}$$

This is the situation of two lasers with different frequencies. With the help of Eq. 1.22, one can obtain

$$\boldsymbol{\mathcal{E}}^* \times \boldsymbol{\mathcal{E}} = E_1 E_2 (e^{-i2k_0 x - i\delta\omega t} - e^{i2k_0 x + i\delta\omega t})\mathbf{e_x}, \tag{1.40}$$

where $\delta\omega = \omega_2 - \omega_1$. Then, atoms in this laser field experience a light-induced Zeeman field as

$$\hat{H}_{\mathrm{eff}} = iu_v E_1 E_2 (e^{-i2k_0 x - i\delta\omega t} - e^{i2k_0 x + i\delta\omega t})\hat{S}_x. \tag{1.41}$$

In the low-field regime, by using the Wigner–Eckart theorem, one can project the Hamiltonian Eq. 1.43 into the hyperfine eigenstate bases, where the $\hat{S}_{x,y,z}$ terms become $\hat{F}_{x,y,z}$

https://doi.org/10.1017/9781108595216.002 Published online by Cambridge University Press

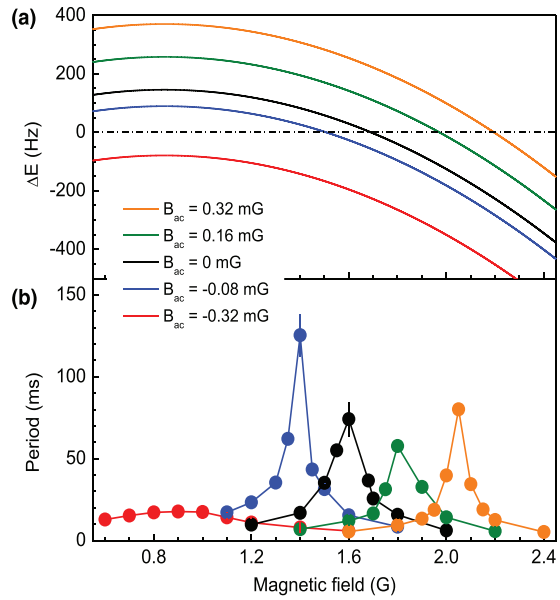

Figure 1.6 Physical effect of the light-induced Zeeman energy. (a) The energy difference between different spin states ΔE defined in Eq. 1.38. (b) The observed spin exchanging oscillation periods as a function of the real magnetic field strength, for different light-induced magnetic fields. B_{ac} in the figure denotes the light-induced Zeeman field for ^{87}Rb at different intensities of the circular polarized light. Reprinted from Figure [108]. A color version of this figure can be found in the resources tab for this book at cambridge.org/zhai.

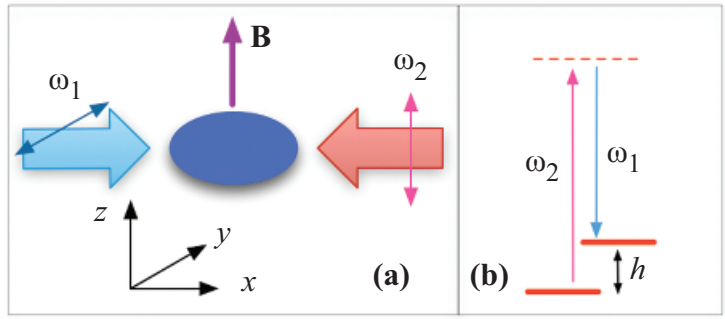

Figure 1.7 Schematic of the synthetic spin-orbit coupling for atoms. (a) The laser configuration of the Raman coupling scheme. Two counterpropagating Raman beams with different polarization directions and different frequencies are applied along $\hat{x}$, and **B** is the real magnetic field applied along the $\hat{z}$ direction. (b) Raman coupling couples two Zeeman levels split by a Zeeman energy denoted by h. A color version of this figure can be found in the resources tab for this book at cambridge.org/zhai.

https://doi.org/10.1017/9781108595216.002 Published online by Cambridge University Press

terms, respectively.[3] Thus, the total Hamiltonian for the spin part contains both the real static Zeeman field and the light-induced Zeeman field as

$$\hat{H}_{\mathrm{s}} = h\hat{F}_z + i\Omega(e^{-i2k_0x-i\delta\omega t} - e^{i2k_0x+i\delta\omega t})\hat{F}_x, \tag{1.42}$$

where Ω denotes the coupling constant proportional to E_1E_2. Let us consider the situation that $\delta\omega$ is near-resonant with h. Following the discussion above, we apply a unitary transformation $\hat{\mathcal{U}} = e^{-i\delta\omega t\hat{F}_z/\hbar}$ and implement the rotating-wave approximation to drop the terms with $2\delta\omega$ frequency; the full Hamiltonian can be reduced to

$$\hat{H}_{\mathrm{s}} = (h-\delta\omega)\hat{F}_z + \Omega(\sin(2k_0x)\hat{F}_x - \cos(2k_0x)\hat{F}_y). \tag{1.43}$$

This Hamiltonian represents a spatially dependent Zeeman field that varies the spin direction at the scale of the laser wavelength.

The discussion above mainly concerns the motion of electrons inside an atom. Now, we consider an atom as a point particle moving in such a spatially dependent Zeeman field, and the Hamiltonian is given by

$$\hat{H} = \frac{\hbar^2\hat{\mathbf{k}}^2}{2m} + \hat{H}_{\mathrm{s}}, \tag{1.44}$$

where $\mathbf{k}$ now stands for the spatial motion of the atom. By applying a spatially dependent spin rotation $\hat{\mathcal{U}} = e^{-i2k_0x\hat{F}_z}$ to the Hamiltonian, one can obtain that

$$\hat{H} = \frac{\hbar^2}{2m}(\hat{k}_x - 2k_0\hat{F}_z/\hbar)^2 + \frac{\hbar^2\,\hat{\mathbf{k}}_\perp^2}{2m} + (h-\delta\omega)\hat{F}_z - \Omega\hat{F}_y. \tag{1.45}$$

Below we will analyze several different situations of the model Eq. 1.45.

- When $h-\delta\omega$ is much larger than Ω, we can only keep the lowest spin branch by implementing the adiabatic approximation. Without loss of generality, we consider $h-\delta\omega > 0$. Nearby the minimum of the dispersion, the dispersion can be well approximated by $\frac{1}{2m^*}(k_x - k_{\min})^2$ [112]. For small Ω, $k_{\min} \approx 2k_0 + o(\Omega)$. This can be viewed as realizing a constant gauge $U(1)$ gauge field $\hat{H} = \frac{1}{2m^*}(k_x - A_x)^2$ where A_x is a constant. A constant $U(1)$ gauge field has no physical effect because there is neither an electric nor a magnetic field, and it can be gauged away by a gauge transformation $e^{ik_{\min}x}$.
- In the regime discussed above, if Ω depends on the y coordinate, then it means $k_{\min}$, or equivalently, to say, A_x, depends on y. This leads to a synthetic magnetic field $B_{\mathrm{syn}} = -\partial A_x/\partial y$ [113]. This emergent synthetic magnetic field can also be understood in terms of spatial twisting of spins by the light-induced magnetic field, as discussed in Section 1.2. If Ω depends on time, then A_x also depends on time. This realizes a synthetic electric field given by $E_{\mathrm{syn}} = -\partial A_x/\partial t$ [115]. However, the spatial and temporal dependences of these gauge fields are completely fixed by the external classical fields, which are the profile of the laser intensity in this case. There is no quantum dynamics of these gauge fields. We will summarize the timeline of simulating various kinds of $U(1)$

[3] According to the Wigner–Eckart theorem, the projection from $\hat{S}_{x,y,z}$ terms to $\hat{F}_{x,y,z}$ terms acquires a constant coefficient given by $\frac{F(F+1)-I(I+1)+J(J+1)}{2F(F+1)}$. For ^{87}Rb, $I = 3/2$, $J = 1/2$, and for the $F = 1$ manifold, this constant is $-1/4$.

https://doi.org/10.1017/9781108595216.002 Published online by Cambridge University Press

gauge fields in Box 7.3, where we will discuss how to realize a $U(1)$ gauge field with its own dynamics.

- In the regime when $h-\delta\omega$ is comparable to Ω, we need to keep all spin components. Here we again consider Ω a constant independent of spatial and temporal coordinates, but we need to keep both the vector gauge potential $A_x = 2k_0\hat{F}_z/\hbar$ and the scalar potential $-\Omega\hat{F}_y$ terms as matrices. These two terms do not commute with each other, and this realizes a non-abelian gauge field. Unlike the abelian case, a non-abelian gauge field has a physical effect even though they are constants. As one can see, if one wants to gauge away the vector potential, one needs to make a gauge transformation $e^{2ik_0x\hat{F}_z}$, and this gauge transformation does not commute with the scalar potential term.

  In this case, the Hamiltonian can also be written as

$$\hat{H} = \frac{\hbar^2\hat{\mathbf{k}}^2}{2m} + \mathbf{h}_\mathbf{k}\cdot\hat{\mathbf{F}}, \tag{1.46}$$

  where

$$\mathbf{h}_\mathbf{k} = \left(0, -\Omega, \left(h - \delta\omega - \frac{\hbar^2}{m}k_0k_x\right)\right). \tag{1.47}$$

  In this way, this Hamiltonian can be viewed as a momentum-dependent Zeeman field. For eigenstates, the spin direction of the atom is locked by its momentum, which gives rise to the spin-orbit coupling effect. Here we should note that one should not confuse this synthetic spin-orbit coupling with the real spin-orbit coupling discussed in atomic structure. For the synthetic spin-orbit coupling, "orbit" refers to the spatial motion of atoms, and "spin" refers to the total spin of an atom. In nature, neutral atoms do not possess the spin-orbit coupling effect, and here it is a synthetic effect generated by the atom–light interaction. The real spin-orbit coupling refers to the fine structure coupling given by nature, where "orbit" means the motion of electrons around the nucleus inside the atom and "spin" refers to the spin of electrons. Nevertheless, from the discussion above, it is interesting to note that generating the synthetic spin-orbit coupling relies on the real spin-orbit coupling.

- We have not included the quadratic Zeeman energy in the discussion above. Considering atoms like ^{87}Rb with $F = 1$, in the moderate magnetic field, there also exists sizable quadratic Zeeman energy denoted by qF_z^2, as discussed in Section 1.2. Especially, let us consider the situation that $h - \delta\omega \approx q \gg \Omega$, such that

$$\delta = h - \delta\omega - q \ll \Omega \tag{1.48}$$

$$h - \delta\omega + q \approx 2q \gg \Omega. \tag{1.49}$$

  In this case, two states with $|F = 1, F_z = 0\rangle$ and $|F = 1, F_z = -1\rangle$ are nearly degenerate, and their energy separation with $|F = 1, F_z = 1\rangle$ is much larger than the coupling. Hence, we introduce a pseudo-spin-1/2 to represent $|F = 1, F_z = 0\rangle$ and $|F = 1, F_z = -1\rangle$ states, described by the Pauli matrices $\boldsymbol{\sigma}$, and ignore $|F = 1, F_z = 1\rangle$. In the spin-1/2 subspace described by the Pauli matrix, the Hamiltonian can be written as

https://doi.org/10.1017/9781108595216.002 Published online by Cambridge University Press

$$\hat{H} = \frac{\hbar^2}{2m}(\hat{k}_x - k_0\sigma_z)^2 + \frac{\hbar^2\,\hat{\mathbf{k}}_\perp^2}{2m} + \frac{\delta}{2}\sigma_z - \Omega\sigma_y, \tag{1.50}$$

where δ denotes $h - \delta\omega - q$. Upon a spin rotation, the Hamiltonian can also be written in the form used most often in literature:

$$\hat{H} = \frac{\hbar^2}{2m}(\hat{k}_x - k_0\sigma_z)^2 + \frac{\hbar^2\hat{\mathbf{k}}_\perp^2}{2m} + \frac{\delta}{2}\sigma_z + \Omega\sigma_x. \tag{1.51}$$

This Hamiltonian has been realized in both Bose condensate [114] and degenerate Fermi gas [181, 32]. The effects of this spin-orbit coupling in ultracold Bose and Fermi gases have been extensively studied in cold atom physics [186]. We will discuss how this synthetic spin-orbit coupling affects the properties of a Bose condensate in Section 4.5.

1.4 Stimulated Raman Adiabatic Passage

In Section 1.3 we have discussed that atoms in their ground state can experience an effective potential due to the two-photon process via intermediate excited states. In this section, we will discuss a dynamical process that can transfer atoms from one low-energy state to another low-energy state, also through a two-photon process via an intermediate state. This is known as Stimulated Raman Adiabatic Passage (STIRAP).

Here we introduce the simplest version of the STIRAP [178]. As shown in Figure 1.8, the two low-energy states are denoted by $|1\rangle$ and $|2\rangle$ with energy E_1 and E_2, and the excited state is denoted by $|e\rangle$ with energy $E_{\rm ex}$. A laser called a "pump laser" couples $|1\rangle$ to $|e\rangle$ with energy $\omega_{\rm p}$ and a time-dependent coupling strength $\Omega_{\rm p}(t)$, and another laser called a "stoke laser" couples $|2\rangle$ to $|e\rangle$ with energy $\omega_{\rm s}$ and a time-dependent coupling strength $\Omega_{\rm s}(t)$. Here it is important to note that the time dependence of $\Omega_{\rm s}(t)$ and $\Omega_{\rm p}(t)$ should be slow enough compared to other time scales. Here we introduce two detunings $\Delta_{\rm p} = E_{\rm ex} - E_1 - \hbar\omega_{\rm p}$ and $\Delta_{\rm s} = E_{\rm ex} - E_2 - \hbar\omega_{\rm s}$, and STIRAP requires $\Delta_{\rm p} = \Delta_{\rm s}$, which will be denoted by Δ below. Therefore, under the rotating wave approximation, the time-dependent Hamiltonian is given by

$$\hat{H}(t) = \hbar|\Psi\rangle\mathcal{H}(t)\langle\Psi|^T, \tag{1.52}$$

where $|\Psi\rangle$ denotes $(|1\rangle, |2\rangle, |e\rangle)$ and $\langle\Psi|^T$ denotes $(\langle 1|, \langle 2|, \langle e|)^T$, and $\mathcal{H}(t)$ is a 3×3 matrix given by

$$\mathcal{H}(t) = \begin{pmatrix} 0 & 0 & \Omega_{\rm p}(t) \\ 0 & 0 & \Omega_{\rm s}(t) \\ \Omega_{\rm p}(t) & \Omega_{\rm s}(t) & \Delta \end{pmatrix}. \tag{1.53}$$

This Hamiltonian can in fact be rewritten as

$$\hat{H}(t) = A(t)\left[\left(\frac{\Omega_{\rm p}(t)}{A(t)}|1\rangle + \frac{\Omega_{\rm s}(t)}{A(t)}|2\rangle\right)\langle e| + \text{h.c.}\right] + \Delta|e\rangle\langle e|, \tag{1.54}$$

https://doi.org/10.1017/9781108595216.002 Published online by Cambridge University Press

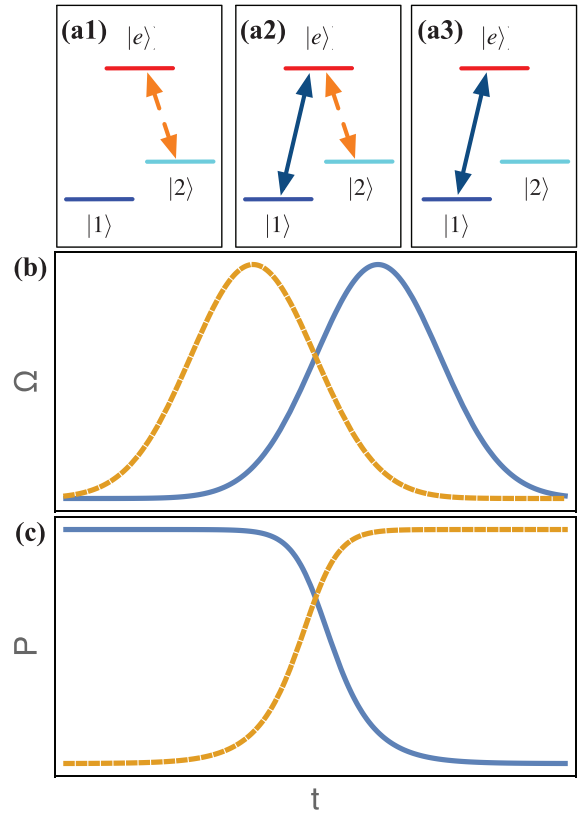

Figure 1.8 Schematic of the STIRAP scheme. (a) How two lasers couple three different states at three different stages. The dashed line and the solid line denote the stoke laser and the pump laser, respectively. (b) The temporal profiles of Ω_s (dashed line) and Ω_p (solid line) as a function of time. (c) The population in the $|1\rangle$ state (solid line) and the population in the $|2\rangle$ state (dashed line) as a function of time. A color version of this figure can be found in the resources tab for this book at cambridge.org/zhai.

where $A(t) = \sqrt{\Omega_p^2(t) + \Omega_s^2(t)}$. Now we define a "bright" state $|B\rangle$ as

$$|B\rangle = \frac{\Omega_p(t)}{A(t)}|1\rangle + \frac{\Omega_s(t)}{A(t)}|2\rangle \tag{1.55}$$

and another "dark state" $|D\rangle$ orthogonal to $|B\rangle$ as

$$|D\rangle = -\frac{\Omega_s(t)}{A(t)}|1\rangle + \frac{\Omega_p(t)}{A(t)}|2\rangle. \tag{1.56}$$

In the Hilbert space spanned by $\{|1\rangle, |2\rangle\}$, only $|B\rangle$ couples to $|e\rangle$, and $|D\rangle$ state does not couple to $|e\rangle$ at all. That is to say, for any given time t, $\mathcal{H}(t)$ can be diagonalized by a unitary matrix $\mathcal{U}(t)$, and there will always be an instantaneous eigenstate $|D(t)\rangle$ whose eigenenergy always remains as zero. The other two instantaneous eigenstates will be in superposition of $|B\rangle$ and $|e\rangle$, and their energies will be $\pm\sqrt{A^2(t) + \Delta^2/4}$.

https://doi.org/10.1017/9781108595216.002 Published online by Cambridge University Press

The key idea of STIRAP relies on this dark state $|D(t)\rangle$. If one solves the time-dependent Schrödinger equation, there will be an extra $i\hbar(\partial_t \mathcal{U}^\dagger(t))\mathcal{U}(t)$ term when one rotates into the instantaneous eigenstate bases, as we discussed in Section 1.3. The off-diagonal matrix elements of this term can couple different instantaneous eigenstates. However, since the three instantaneous eigenstates are always separated by a finite energy difference, if $\mathcal{H}(t)$ changes sufficiently smoothly as a function of time, $\mathcal{U}(t)$ also varies sufficiently smoothly, and therefore the off-diagonal matrix elements can be made sufficiently small compared with the energy separation of the three instantaneous eigenstates. Therefore, in this adiabatic regime, the system can nearly remain in one of the instantaneous eigenstates during the time evolution. In this case of STIRAP, we would like to keep the system in the dark state $|D(t)\rangle$.

The idea of the STIRAP is to utilize the dark state $|D(t)\rangle$ to transfer atoms from $|1\rangle$ to $|2\rangle$ by properly designing the time dependence of $\Omega_p(t)$ and $\Omega_s(t)$. To fulfill this goal, at initial time, $\Omega_p/\Omega_s \to 0$ and therefore $|D\rangle \to |1\rangle$; and at the final time of the transfer, $\Omega_s/\Omega_p \to 0$ and therefore $|D\rangle \to |2\rangle$. The time sequence is very counterintuitive. It basically constitutes three steps: (1) initially, atoms are populated in state $|1\rangle$, however, one first opens up the coupling between $|2\rangle$ and $|e\rangle$, as shown in Figure 1.8(a1); (2) in the intermediate stage, both lasers' coupling is open, and atoms are transferred from $|1\rangle$ to $|2\rangle$, as shown in Figure 1.8(a2); and (3) when atoms have been gradually transferred to the $|2\rangle$ state, the coupling between $|e\rangle$ and the less occupied $|1\rangle$ should remain open, as shown in Figure 1.8(a3). We schematically show an example of the temporal profiles of $\Omega_s(t)$ and $\Omega_p(t)$ in Figure 1.8(b). Correspondingly, the populations of the $|1\rangle$ state and $|2\rangle$ state are given by $\Omega_s^2(t)/A^2(t)$ and $\Omega_p^2/A^2(t)$, respectively, and they are plotted in Figure 1.8(c).

The STIRAP scheme transfers atoms from one state to another in a coherent way, and the energy difference between these two states is taken away by photons such that there is no inelastic energy transfer. The STIRAP scheme has two major advantages that make the STIRAP scheme very stable:

- Because this dark state does not involve the excited state component $|e\rangle$, it is stable against the spontaneous emission of the $|e\rangle$ state.
- This scheme is not sensitive to the details of the temporal profile of $\Omega_p(t)$ and $\Omega_s(t)$, and it works as long as the temporal profiles satisfy the aforementioned initial and long time conditions.

STIRAP has been widely used in atomic and molecular physics, as well as chemistry [178]. In cold atom physics, STIRAP has been mostly used for producing ultracold ground state molecules [127]. In this application, it transfers the two-body molecular state instead of the single-particle atomic states, but the working principle is the same as discussed above. The experiment starts with an ultracold sample of the Feshbach molecules whose energy is very close to scattering threshold, and the size is as large as the interparticle spacing. The Feshbach molecule will be discussed in Section 2.4. The goal is to transfer them into the ground state molecule, whose energy is more than 10^{14}Hz below the threshold, and the size of the molecule is a few times the Bohr radius. This process is shown in Figure 1.9. In this case, the excited state is chosen as one of the excited molecular states that has reasonably large coupling matrix elements with both the initial Feshbach molecule

https://doi.org/10.1017/9781108595216.002 Published online by Cambridge University Press

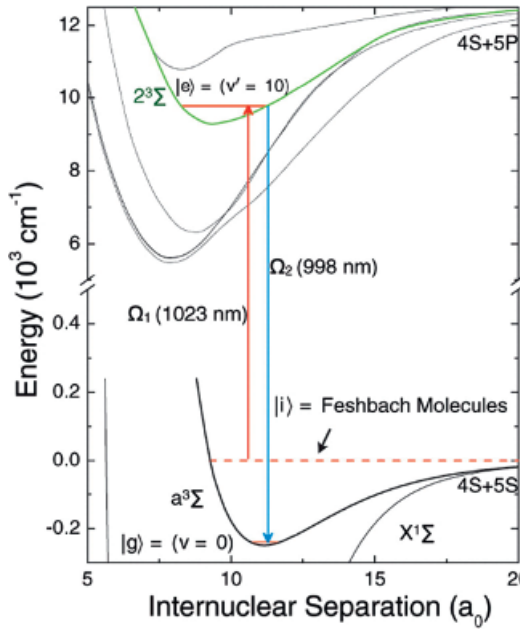

Figure 1.9 STIRAP for producing ground-state molecules. Schematic of using the STIRAP method to transfer a molecule from a Feshbach molecule to the ground state molecule through a molecular excited state. Reprinted from Ref. [127]. A color version of this figure can be found in the resources tab for this book at cambridge.org/zhai.

and the final ground state molecule. The transfer efficiency can be larger than 90%. As the STIRAP process is coherent, the final sample of the ground state molecules remains at very low temperature. Using this method, a degenerate gas of ground state molecules has been produced [45].

Exercises

1.1 Considering an electron with Coulomb interaction between electron and nucleus, the Hamiltonian is given by

$$\hat{H} = -\frac{\hbar^2 \nabla_i^2}{2m^*} - \frac{Z\kappa}{r}, \tag{1.57}$$

and considering the Laplace–Runge–Lene vector defined as

$$\hat{\mathbf{J}} = \frac{1}{2m^*}\left(\hat{\mathbf{p}} \times \hat{\mathbf{L}} - \hat{\mathbf{L}} \times \hat{\mathbf{p}}\right) - Z\kappa \frac{\mathbf{r}}{r}. \tag{1.58}$$

Show that $[\hat{\mathbf{J}}, \hat{H}] = 0$. This operator $\hat{\mathbf{J}}$ and the angular momentum operator $\hat{\mathbf{L}}$ together form the $SO(4)$ algebra. This only works for the Coulomb potential.

https://doi.org/10.1017/9781108595216.002 Published online by Cambridge University Press

1.2 Considering the excited state of the alkali-metal atom with $L = 1$ and $S = 1/2$, write down the eigenstates for a Hamiltonian with spin-orbit coupling

$$\mathbf{H} = \alpha_{\mathrm{f}} \hat{\mathbf{S}} \cdot \hat{\mathbf{L}}, \tag{1.59}$$

where α_{f} is a constant.

1.3 Considering a ^{87}Rb or ^{6}Li atom in magnetic field $B\hat{z}$, the Hamiltonian can be written as Eq. 1.6.

(1) Solve the full energy spectrum E as a function of B.
(2) Analyze how E depends on B for small B, and find both the linear and the quadratic Zeeman shifts. For the linear Zeeman field, one can also use the Wiger–Eckart theorem to determine the coefficient g_{F}.
(3) Analyze the spin structure at large B.

1.4 Show that in a regime without electric current, the magnetic field strength can not have a local maximum.

1.5 Estimate the regime where the Majorana transition becomes significant for ^{87}Rb atoms in a pure quadrupole trap with $\mathbf{B} = B_0(x, y, -2z)$.

1.6 Derive Eq. 1.19 following the rotating wave approximation.

1.7 Considering the Hamiltonian Eq. 1.42,

(1) show, by using the rotating wave approximation with $\hat{\mathcal{U}} = e^{-i\delta\omega t\hat{F}_z/\hbar}$, that the Hamiltonian can be reduced to the form of Eq. 1.43.
(2) show, by using a unitary transformation $\hat{\mathcal{U}} = e^{-i2k_0x\hat{F}_z}$, that the Hamiltonian Eq. 1.43 can be mapped to Eq. 1.51.

1.8 Considering a time-dependent Hamiltonian

$$\hat{H} = \omega\hat{F}_z + B_0\cos(\omega_0 t)\hat{F}_x, \tag{1.60}$$

show that when ω_0 is close to ω, by rotating wave approximation, the Hamiltonian can become a time-independent one as

$$\hat{H} = \Delta\hat{F}_z + \frac{B_0}{2}\hat{F}_x, \tag{1.61}$$

where $\Delta = \omega - \omega_0$.

1.9 Considering a Hamiltonian with four coupled states $|0\rangle$, $|1\rangle$, $|2\rangle$, and $|3\rangle$,

(1) construct a Hamiltonian that exhibits two dark states. Write down the wave function of these two dark states.
(2) discuss the condition when this Hamiltonian has one dark state.

https://doi.org/10.1017/9781108595216.002 Published online by Cambridge University Press